ELSEVIER

Earth and Planetary Science Letters 210 (2003) 151–165

EPSL

www.elsevier.com/locate/epsl

The marine $^{187}Os/^{188}Os$ record of the Eocene–Oligocene transition: the interplay of weathering and glaciation

G. Ravizza [a,*], B. Peucker-Ehrenbrink [b]

[a] *Department of Geology and Geophysics, Woods Hole Oceanographic Institution, Woods Hole, MA 02543, USA*
[b] *Department of Marine Chemistry and Geochemistry, Woods Hole Oceanographic Institution, Woods Hole, MA 02543, USA*

Received 12 July 2002; received in revised form 14 February 2003; accepted 13 March 2003

Abstract

Osmium (Os) isotope analyses of bulk sediments from the South Atlantic, Equatorial Pacific, and the Italian Apennines yield a well-dated and coherent pattern of $^{187}Os/^{188}Os$ variation from the late Eocene to the early Oligocene. The resulting composite record demonstrates the global character of two prominent features of the low-resolution LL44-GPC3 Os isotope record [Pegram and Turekian, Geochim. Cosmochim. Acta 63 (1999) 4053–4058]. These are: (1) a pronounced minimum in $^{187}Os/^{188}Os$ (0.22–0.27) in the late Eocene, between 34 and 34.5 Ma, and (2) a subsequent rapid increase in $^{187}Os/^{188}Os$, to approximately 0.6 by 32 Ma. An ultramafic weathering event and an increased influx of extraterrestrial particles to the Earth are discussed as alternative explanations for the late Eocene $^{187}Os/^{188}Os$ minimum. Comparison of the $^{187}Os/^{188}Os$ to benthic foraminiferal oxygen isotope records demonstrates that the nearly three-fold increase in $^{187}Os/^{188}Os$ from the late Eocene minimum coincides with the growth and decay of the first large ice sheet of the Oligocene (Oi1 [Miller et al., J. Geophys. Res. 96 (1991) 6829–6848]). The fine structure of the Os isotope record indicates that enhanced release of radiogenic Os, unrelated to the recovery from late Eocene minimum, lagged the initiation of the Oi1 event by roughly 0.5 Myr. This record, in conjunction with weathering studies in modern glacial soils [Blum, in: W.F. Ruddiman (Ed.), Tectonic Uplift and Climate Change, Plenum Press, New York, 1997, pp. 259–288; Peucker-Ehrenbrink and Blum, Geochim. Cosmochim. Acta 62 (1998) 3193–3203], suggests that exposure of freshly eroded material during deglaciation following Oi1 enhanced chemical weathering rates, and may have contributed to ice sheet stabilization by drawing down atmospheric carbon dioxide. The improved temporal resolution and age control of the refined Eocene–Oligocene Os isotope record also makes it possible to illustrate the late Eocene Os isotope excursion as a tool for global correlation of marine sediments.

Keywords: Eocene; Oligocene; Glaciation; Osmium isotopes; Weathering; Extraterrestrial influx; Ultramafic; Paleoceanography

1. Introduction

The Eocene–Oligocene (E–O) transition marks the end of Eocene warmth and the onset of major glaciation in Antarctica [5]. In the late Eocene there were at least two large extraterrestrial impacts [6,7] and a more protracted episode of in-

* Corresponding author. Present address: Department of Geology and Geophysics, University of Hawaii, Honolulu, HI 96822-2225, USA.
E-mail addresses: ravizza@hawaii.edu (G. Ravizza), behrenbrink@whoi.edu (B. Peucker-Ehrenbrink).

0012-821X/03/$ – see front matter © 2003 Published by Elsevier Science B.V.
doi:10.1016/S0012-821X(03)00137-7

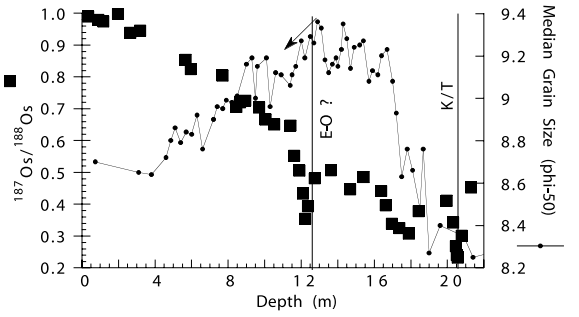

Fig. 1. Cenozoic marine $^{187}Os/^{188}Os$ record preserved in LL44-GPC3 [1], a North Pacific pelagic clay sequence and eolian grain size [55] plotted versus depth in core. The trend of increasing eolian grain size (small ϕ-50 values) that begins in the late Eocene (arrow) is interpreted as evidence of increasingly vigorous atmospheric circulation [55]. Note the pronounced excursion to low $^{187}Os/^{188}Os$ just above the putative E–O boundary at 12 m depth. New data reported here (Fig. 2 and 3) show that this minimum occurs in the late Eocene at 34.2 Ma, requiring that the transition to increasing eolian grain size precede major Antarctic glaciation (33.6 Ma) by several hundred thousand years. The E–O boundary shown is defined by ichthyolith biostratigraphy [56].

creased cosmic dust flux [8]. Both Antarctic glaciation and an increased influx of extraterrestrial material could have caused significant changes in the $^{187}Os/^{188}Os$ of seawater. The North Pacific pelagic clay core, LL44-GPC3, provides the best available overview of Cenozoic variability in the marine osmium isotope record [1,9]. A large excursion to low $^{187}Os/^{188}Os$ close to the E–O boundary is one of the most prominent features of this record (Fig. 1). The asymmetric shoulders of the excursion are equally important in that they define a significant and permanent increase in the $^{187}Os/^{188}Os$ of seawater, from values between 0.45 and 0.5 before the excursion to values greater than 0.6 after the excursion. These large variations in the LL44-GPC3 Os isotope record provide the impetus for a more detailed study of this important climate transition.

This study has two main objectives. The first is to better establish the timing and geographic extent of the E–O Os isotope excursion that is recorded in LL44-GPC3. Specifically, we test the hypothesis that the increased influx of extraterrestrial material in the late Eocene [8] was synchronous with the excursion to low $^{187}Os/^{188}Os$ ratios close to the E–O boundary. The combined LL44-GPC3 He–Os isotope record suggests that they are not [9], but this single core need not be representative of either global ^{3}He flux or seawater $^{187}Os/^{188}Os$. The second objective is to compare seawater $^{187}Os/^{188}Os$ variations across the E–O transition to the history of ice volume changes recorded by $\delta^{18}O$ in benthic foraminifers in order to establish leads and lags between these two paleoceanographic records. If shifts to heavier oxygen isotope composition, indicating increased ice volume, precede rising $^{187}Os/^{188}Os$, then this is supportive of the hypothesis that glaciation, either directly or indirectly, enhanced continental weathering [10–12]. Alternatively, if oxygen isotope shifts lag the increase in seawater $^{187}Os/^{188}Os$, then this is consistent with the hypothesis that increased chemical weathering fluxes preceded major Cenozoic glaciation, and may have played a causative role in climate change by drawing down atmospheric CO_2 [13,14]. In addition to these two main objectives, refinements of the E–O marine Os record we report here also provide the age control necessary to illustrate the potential of Os isotopic chemostratigraphy in pelagic clays.

Sediments from the South Atlantic, the Equatorial Pacific, and the Massignano section in the Italian Apennines were investigated to construct a more detailed record of $^{187}Os/^{188}Os$ variations across the E–O transition. The Massignano section was selected for this study because previous studies of impact debris [15,16] and ^{3}He [8] allow direct comparison of Os isotope variations to records of extraterrestrial influx. South Atlantic sediments from Deep Sea Drilling Project (DSDP) Site 522 were investigated so that Os isotope data could be compared to existing stable isotope data from the same core [5]. Metalliferous sediments from the Equatorial Pacific, DSDP Hole 574C, were included in this study because Os isotope analyses of lithologically similar sediments have consistently yielded reliable data for reconstructing past variations in the Os isotopic composition of seawater [17–20]. In all three localities biostratigraphic data constrain the sediment sequences to span the E–O boundary. Using biostratigraphic data and magnetostratigraphy to correlate between these sediment sequences, a

composite record of Os isotope variation from the late Eocene to the early Oligocene is constructed.

2. Sample material

2.1. Massignano samples

The Massignano section is located in the Umbria–Marche basin in the northeastern portion of the Italian Apennines. Lithologically the Massignano section is comprised of marly limestones with a lesser proportion of calcareous marl. $CaCO_3$ content varies from 50 to 80 wt% [21]. There are three key reasons we chose to investigate Os isotope variations in this section. First, there is a large body of integrated stratigraphic data available to constrain the age model for the Massignano section because it is the Global Stratotype Section and Point for the E–O boundary [22]. Second, several detailed studies have been conducted documenting the distribution of impact-related material at Massignano [15,16,21]. These studies provide marker horizons attributable to the late Eocene impact events at Popigai [6] and Chesapeake Bay [7]. Third, a detailed investigation of He concentrations and isotope variations in these sediments revealed evidence of an episode of increased cosmic dust flux lasting roughly 2 Myr [8]. We analyzed splits of sample powders remaining from the He isotope study cited above. These samples included both outcrop samples and drill core material. The detailed magnetostratigraphy of the Massignano section [23] provides the basis of a robust age model.

2.2. DSDP Site 522

This core was recovered from the Angola Basin in the South Atlantic (26°6.843′S, 5°7.784′W; 4400 m). The sediments recovered from Site 522 from 120 to 147 m below seafloor (mbsf) are of late Eocene to early Oligocene age. Over this depth interval the sediments are 85–95 wt% $CaCO_3$, faintly yellow-brown colored, and are classified as nannofossil to foram–nannofossil oozes [24]. The two principal reasons for investigating sediments from Site 522 are the excellent age control provided by magnetostratigraphy [25] and the detailed benthic foraminiferal stable isotope record for this site [5]. Recent Mg/Ca analyses of benthic foraminifers from this core [26] support the interpretation that variation in the $\delta^{18}O$ benthic foraminiferal record largely reflects changes in ice volume rather than temperature. Thus the Site 522 record provides an opportunity to compare seawater $^{187}Os/^{188}Os$ variations to changes in ice volume during the first major Oligocene glaciation [2].

2.3. DSDP Hole 574C

The site is located in the Equatorial Pacific (4°12.52′N, 133°19.81′W; 4561 m) on oceanic crust of late Eocene age. The lowermost sediment unit recovered from this site is comprised of metalliferous chalk and spans the E–O boundary [27]. This lithology has been shown to accurately record the $^{187}Os/^{188}Os$ of modern seawater and demonstrated to record past variations in the Os isotopic composition of seawater [17–20]. The lithologic suitability of the Hole 574C E–O sediments was the main reason these sediments were studied here. Age control for these sediments is inferior to Massignano and Site 522 sites because this site lacks a reliable magnetostratigraphy. The best constrained biostratigraphic indicator of the E–O boundary in terms of depth range is the last occurrence of the benthic foraminifer *Nuttallides truempyi* at 506 mbsf [28]. Other biostratigraphic horizons, nannofossil [29] diatoms [30], and radiolarians [31] are consistent with this assignment within 1–2 m depth in the core. The planktonic foraminiferal record suggests a deeper placement for the E–O boundary, but this is likely compromised by carbonate dissolution artifacts [28].

3. Methods

Os isotope analyses of bulk sediments were performed by introducing OsO_4 vapor directly into a magnetic-sector inductively coupled plasma mass spectrometer (ICP-MS) as described by Hassler et al. [32]. These isotope ratio measurements followed preconcentration of Os and the other plat-

inum group elements by NiS fire assay [33]. Approximately 5 g of sediment was fused for each analysis. Though the ICP-MS method for Os isotope analysis is less sensitive and less precise than Os isotope analysis by negative thermal ionization mass spectrometry (NTIMS), it is much less time-consuming. The relative speed of ICP-MS Os isotope analyses makes this method well-suited for investigating the marine Os isotope record because the dynamic range in $^{187}Os/^{188}Os$ is large and numerous analyses are required. Approximately one-third of the 55 samples investigated were analyzed in duplicate. Platinum, Pd, and Ir concentrations were determined on the same powder splits used for Os isotope analyses. These data will be reported separately. Rhenium concentrations were determined in a small subset of samples by isotope dilution ICP-MS following acid digestion of a separate powder split and purification using anion exchange resin.

Repeated analyses of an in-house Os standard solution yielded an average $^{187}Os/^{188}Os$ of 0.1736 ± 0.0009 (1 S.D.; $n = 35$). This value agrees well with the value previously established for this solution by NTIMS (0.1741 ± 0.0002 [32]). Based on eight analyses of sample-free fusions, procedural blanks for the Os analyses were 1.8 ± 0.8 pg Os/g sample with a $^{187}Os/^{188}Os$ of 0.46 ± 0.11 (both 1 S.D.) The resulting blank corrections to the measured Os concentrations averaged 3.8% and were not larger than 9%. Procedural blanks ($n = 4$) for the Re analyses were all less than 2 pg total analyte.

4. Results and discussion

Measured Os concentrations in the samples investigated range from 20 to 164 pg/g (Table 1), similar to concentrations reported previously for pelagic carbonates [20,34]. Measured Re concentrations range from 13 to 439 pg/g (Table 1), and resulting $^{187}Re/^{188}Os$ ratios range from 0.5 to 40. Corrections for the in situ production of ^{187}Os by ^{187}Re decay were not applied because they are so small as to be negligible, averaging 0.1% with a maximum correction of 0.5%.

In all three of the records investigated $^{187}Os/^{188}Os$ displays a pronounced minimum in the late Eocene (Fig. 2). The lowest $^{187}Os/^{188}Os$ in each core falls in the range 0.22–0.27, lower than the lowest $^{187}Os/^{188}Os$ measured in the E–O excursion in LL44-GPC3 (0.35 [1]). Note that in Fig. 2a three analyses distributed over the top 50 cm of core 37 from Site 522 (Table 1) were not plotted. Samples from these three depth intervals define an excursion to high $^{187}Os/^{188}Os$ that reaches a maximum value of 2.9, a ratio nearly three times larger than that of average continental crust. At this time we believe that these unusually large ratios result from local contamination with radiogenic Os during the coring operation. The fact that no comparable excursion was found in samples from Site 574, sampled at 50 cm intervals, supports this interpretation. Additional work is underway to examine this possibility more carefully.

A composite record showing $^{187}Os/^{188}Os$ variations as a function of age (Fig. 3) was constructed using measured $^{187}Os/^{188}Os$ ratios (Fig. 2 and Table 1) and models describing the age–depth relationship in each of the three sediment sequences. For Massignano and Site 522 we have used the same age models as used in the ^{3}He study of Farley et al. [8] and Zachos et al. [5], respectively. The age–depth model for Hole 574C is less well-constrained than those of the two other sites because there is not a reliable magnetostratigraphy, and there are significant gaps in core recovery. To relate depth in core to absolute age we have used an age model which sets the E–O boundary at 506 mbsf [28] and assumes a constant sedimentation rate of 1.33 cm/kyr.

Between 34 and 34.5 Ma, all three records display a pronounced excursion to very low $^{187}Os/^{188}Os$ (0.22–0.27) from higher late Eocene $^{187}Os/^{188}Os$ (0.4–0.45). Following the local minimum, $^{187}Os/^{188}Os$ rises rapidly to approximately 0.6 by 32.5 Ma. The high $^{187}Os/^{188}Os$ in the early Oligocene relative to late Eocene imparts a gross asymmetry to this composite record. Both the late Eocene $^{187}Os/^{188}Os$ excursion and the asymmetry about this minimum are also apparent in the low-resolution LL44-GPC3 record (Fig. 1) of Pegram and Turekian [1]. Based on the overall coherence of the three new records to one another

and the GPC3 record, we argue that these data reflect large changes in the $^{187}Os/^{188}Os$ of seawater across the E–O transition. Among the three data sets, the Massignano data are consistently lower in $^{187}Os/^{188}Os$ than the other two sites. The cause of this offset is uncertain. While it is possible that E–O seawater was isotopically heterogeneous with respect to Os, it is equally likely that the Os isotopic composition of the Massignano samples is influenced by a non-hydrogenous Os component that biases these samples to $^{187}Os/^{188}Os$ ratios lower than that of contemporaneous seawater. Given this uncertainty we emphasize only the two most prominent features of this record noted above: (1) an excursion to low $^{187}Os/^{188}Os$ values between 34.2 and 34.3 Ma, and (2) the Os isotopic contrast between the early Oligocene ($^{187}Os/^{188}Os \approx 0.6$) and the late Eocene samples ($^{187}Os/^{188}Os$: 0.4–0.45).

4.1. The late Eocene $^{187}Os/^{188}Os$ minimum

In principle the excursion to very low seawater $^{187}Os/^{188}Os$ in the late Eocene could result from either a diminished supply of radiogenic Os to the ocean, or an increased supply of unradiogenic Os. Two lines of evidence indicate that the latter is more likely than the former. First, model calculations indicate that to achieve a seawater $^{187}Os/^{188}Os$ ratio as low as 0.25 solely by decreasing the influx of radiogenic Os from continental erosion would require an unreasonably large decrease in riverine Os flux to the ocean. Second, calculated Os burial fluxes from the three sediment sequences studied here indicate that the late Eocene Os isotope minimum was characterized by more rapid Os burial, consistent with increased Os influx to the ocean. Both of these points are discussed below.

4.1.1. Reduced radiogenic Os flux

Interpreting the very low $^{187}Os/^{188}Os$ of late Eocene seawater as the result of variable flux of radiogenic continental Os against a more constant unradiogenic input, is analogous to the interpretation of Cenozoic rise in seawater $^{87}Sr/^{86}Sr$ made in previous studies [14,35]. However, interpreting the brief late Eocene Os isotope excursion in this way implies a large decrease in radiogenic Os from continental weathering for several hundred thousand years. To calculate the magnitude of the perturbation in the marine Os isotope cycle required to produce the late Eocene Os isotope excursion, we estimated the Eocene marine Os isotope balance prior to the excursion based on two simple assumptions. First, following Wallmann [36], we assumed that total riverine flux of Os to the ocean in the late Eocene is reduced to 30% of the present-day flux (Table 2, Paleogene 1). Second, to achieve a steady-state seawater $^{187}Os/^{188}Os$ ratio of 0.45 with this reduced river flux and hydrothermal input of Os equivalent to modern estimates, the $^{187}Os/^{188}Os$ of Eocene riverine input must also decrease to approximately 0.81 from 1.4 (Table 2, Paleogene 2). Other recent formulations of the present-day marine Os budget yield somewhat different results [37,38]. However, the fractional decrease in late Eocene riverine $^{187}Os/^{188}Os$ relative to estimated modern values is similar, varying between 37% and 47%, regardless of which estimate of present-day riverine $^{187}Os/^{188}Os$ is used in the calculation. Using Paleogene 2 (Table 2) as our best estimate for Os isotope balance, the supply of radiogenic Os to the ocean must decrease to 30% of pre-excursion levels for roughly 200 kyr to produce the late Eocene minimum in seawater $^{187}Os/^{188}Os$ (Fig. 4, model curve 1). This corresponds to a 95% reduction in riverine Os flux relative to modern inputs. We contend that such a large decrease is unreasonable.

4.1.2. Increased Os burial fluxes

Calculated Os burial fluxes (Table 3) from the three sediment sequences investigated here show that the late Eocene minimum in seawater $^{187}Os/^{188}Os$ is associated with increases in the rate of Os burial and not decreases (Fig. 5A). Given the short marine residence time of Os, these increases in burial flux are suggestive of increased Os supply to the ocean. The second model curve in Fig. 4 assumes the pre-excursion steady-state conditions (R_{ss} and $^{188}F_{ss}$, total ^{188}Os flux in mol/yr) identical to those outlined in the preceding paragraph (Table 2, Paleogene 2). This background flux of Os is augmented by a variable, additional

Table 1
Results of Os isotope analyses of sediments from Massignano, DSDP 574C (Equatorial Pacific) and DSDP 522 (South Atlantic)

Sample name	Depth (m)	Age (Ma)	$^{187}Os/^{188}Os$	$\pm 2\sigma$	Os (pg/g)	Re (pg/g)
Massignano						
M12	4.72	35.82	0.332	0.012	103	36
M12 (dup.)			0.444	0.005	55	19
M14	5.55	35.70	0.466	0.008	44	40
M14 (dup.)			0.403	0.008	60	
M20	6.49	35.56	0.477	0.007	62	
Mac 97 32.5	7.5	35.41	0.443	0.010	51	
M27	9.65	35.08	0.438	0.012	59	
M31	11.68	34.78	0.358	0.011	82	24
M31 (dup.)			0.379	0.011	87	
Mac 97 25.45	13.6	34.49	0.253	0.007	160	58
Mac 97 25.45 (dup.)			0.2504	0.0017	159	
Mas 97 15.40	15.4	34.22	0.220	0.005	160	22
Mas 97 15.40 (dup.)			0.291	0.003	119	17
Mac 97 20.45	17.93	33.84	0.344	0.004	98	175
Mac 97 20.45 (dup.)			0.330	0.011	113	
Mac 97 16.99	20.92	33.40	0.383	0.009	90	
Mac 97 13.90	23.6	32.99	0.406	0.005	55	439
Mac 97 13.90 (dup.)			0.431	0.012	69	436
	(mbsf)					
DSDP 574C						
574C-033R-01W-103–106cm	499.53	33.38	0.476	0.004	51	
574C-033R-02W-93–96cm	500.93	33.48	0.475	0.011	67	
574C-033R-03W-50–53cm	502	33.56	0.473	0.006	46	
574C-033R-03W-102–105cm	502.52	33.60	0.468	0.004	50	
574C-033R-04W-48–52cm	503.48	33.68	0.464	0.007	61	
574C-033R-04W-48–52cm (dup.)			0.459	0.021	65	
574C-033R-04W-98–102cm	503.98	33.71	0.462	0.003	76	
574C-033R-04W-98–102cm (dup.)			0.490	0.005	64	
574C-033R-04W-146–150	504.46	33.75	0.400	0.014	32	
574C-033R-04W-146–150 (dup.)			0.420	0.005	30	42
574C-033R-05W-48–52cm	504.98	33.79	0.361	0.003	49	
574C-033R-05W-118–122cm	505.68	33.84	0.376	0.009	56	
574C-034R-01W-48–52cm	508.48	34.05	0.364	0.006	31	39
574C-034R-01W-98–102cm	508.98	34.09	0.335	0.007	36	24
574C-034R-01W-146–150cm	509.46	34.12	0.316	0.005	35	
574C-034R-02W-48–52cm	509.98	34.16	0.291	0.006	46	
574C-034R-02W-98–102cm	510.48	34.20	0.266	0.007	47	13
574C-035R-01W-8–12cm	517.58	34.73	0.410	0.008	26	
574C-035R-01W-118–122cm	518.68	34.81	0.415	0.020	20	
DSDP 522						
73-522-032-01W-87	122.67	32.44	0.593	0.013	22	
73-522-032-01W-87 (dup.)			0.620	0.018	23	
73-522-032-02W-85	124.15	32.60	0.611	0.014	22	
73-522-32H-3W-76–78	125.52	32.74	0.572	0.009	21	
73-522-32H-3W-76–78cm (dup.)			0.575	0.015	21	
73-522-033-01W-33	127.13	32.92	0.550	0.025	28	
73-522-33H-1W-133–135cm	128.13	33.02	0.557	0.006	19	
73-522-033-02W-93	129.23	33.12	0.484	0.020	28	
73-522-034-02W-49	131.96	33.35	0.493	0.012	29	
73-522-034-02W-144	132.64	33.41	0.469	0.009	55	
73-522-034-02W-144 (dup.)			0.465	0.015	25	

Table 1 (*Continued*).

Sample name	Depth (mbsf)	Age (Ma)	$^{187}Os/^{188}Os$	$\pm 2\sigma$	Os (pg/g)	Re (pg/g)
73-522-35H-1W-28–30cm	133.98	33.52	0.608	0.007	37	
73-522-35H-1W-28–30cm (dup.)			0.501	0.012	27	
73-522-035-01W-126	134.96	33.59	0.494	0.009	38	
73-522-035-01W-126 (dup.)			0.451	0.021	20	
73-522-036-01W-43	136.63	33.72	0.466	0.016	21	
73-522-036-01W-43 (dup.)			0.604	0.025	26	
73-522-036-01W-129	137.49	33.79	0.402	0.008	33	
73-522-036-02W-65–67	138.35	33.85	0.397	0.010	28	
73-522-036-02W-122	138.92	33.90	0.393	0.012	41	
73-522-036H-03W-32–35	139.46	33.94	0.377	0.007	35	
73-522-36H-3W-44–48cm	139.58	33.95	0.361	0.003	43	
73-522-36H-3W-44–48cm (dup.)			0.365	0.011	39	
73-522-37H-1W-3–5cm	139.73	33.96	1.038	0.012	66	
73-522-37H-1W-22–25cm	139.92	33.97	2.906	0.031	111	
73-522-037-01W-50	140.2	34.00	0.691	0.011	54	
73-522-037-01W-50 (dup.)			0.681	0.007	52	
73-522-37H-1W-85–87cm	140.55	34.02	0.351	0.006	62	
73-52-037-01W-93–95	140.63	34.03	0.309	0.004	63	
73-522-01W-143–145	141.13	34.07	0.298	0.003	64	
73-522-037-02W-34	141.54	34.10	0.279	0.008	77	
73-522-037-03W-22	142.92	34.20	0.271	0.007	164	
73-522-037-03W-22 (dup.)			0.268	0.004	73	
73-522-038-01W-45	144.15	34.30	0.283	0.008	60	
73-522-038-02W-21	145.41	34.39	0.312	0.004	66	
73-522-038-03W-6	146.76	34.50	0.379	0.018	51	

flux of unradiogenic Os ($^{188}F_{xs}$), $^{187}Os/^{188}Os = 0.13$ (R_{xs}) in order to match the observed seawater record (R_{sw}) using the simple equation:

$$R_{sw} = (^{188}F_{ss}(R_{ss}) + {}^{188}F_{xs}(R_{xs}))/(^{188}F_{ss} + {}^{188}F_{xs})$$

This calculation can be viewed as the opposite of model 1 because seawater $^{187}Os/^{188}Os$ ratios are decreased by an increased supply of unradiogenic Os to the ocean rather than a diminished supply of radiogenic Os. Under this set of assumptions total Os flux to the ocean increases by slightly more than a factor of two at the nadir of the Os isotope excursion. This increase in Os input is similar to the increase in Os burial flux at Massignano and Site 522 during the Os isotope excursion (Fig. 5A). Though Os burial at any specific location need not provide a representative picture of temporal changes in Os removal from the whole ocean, the fact that the lowest $^{187}Os/^{188}Os$ ratios at all three sites are associated with local maxima in Os burial flux (Fig. 5B) indicates that the late Eocene minimum in seawater $^{187}Os/^{188}Os$ is best interpreted as an episode of increased influx of unradiogenic Os to seawater.

4.1.3. Sources of unradiogenic Os

Increased hydrothermal input, increased influx/dissolution of cosmic dust, and chemical weathering of terranes rich in unradiogenic Os on the continents are all possible sources of unradiogenic Os. We consider the latter two possibilities in greater detail below, emphasizing two important constraints that these new data place on the timing and duration of the late Eocene Os isotope excursion. First, $^{187}Os/^{188}Os$ minimum immediately precedes the gradual increase in the benthic foraminiferal oxygen isotope ratios that culminates in the first large ice sheet of the Oligocene (Oi1) glacial event (Fig. 2a). This raises the possibility that this Os isotope excursion may result from processes that played a causative role in climate change across the E–O transition. Second, the duration of the excursion is slightly longer

than 1 Myr; too long for an impact event, but relatively brief compared to the time scales typically associated with tectonic events.

4.1.3.1. Ultramafic weathering. The new constraints on the timing and duration of the negative Os isotope excursion allow us to elaborate on and modify Turekian and Pegram's [9] initial interpretation of this feature of the Cenozoic marine Os isotope record. These workers argued that weathering of ophiolite sequences, known to contain large proportions of Os-rich ultramafic rocks, uplifted by closure of the Tethys, was the primary cause of the abrupt drop in seawater $^{187}Os/^{188}Os$. Though they discussed the potential connection between this Os isotope excursion and climatic changes indicated by the benthic foraminiferal oxygen isotope record, uncertainties in correlating these two paleoceanographic records hampered detailed interpretation. The Site 522 record tightly constrains the relationship between the oxygen and Os isotope records (Fig. 2a). If ophiolite weathering is responsible for producing the documented Os isotope excursion, these new data require that this was a relatively short-lived weathering 'event'.

The timing of the proposed ophiolite weathering event is noteworthy in that it lends support to the hypothesis advanced by Reusch and Maasch [39] that uplift of accreted island arc terranes enhances CO_2 consumption by chemical weathering, leading to cooling and glaciation. These workers proposed that arc erosion would culminate in weathering of ultramafic rocks from the base of the overriding plate, producing a negative excursion in the Os isotope record similar to the late Eocene excursion. In the context of this hypothesis the relatively low seawater $^{87}Sr/^{86}Sr$ of the Eocene [40] can be attributed in part to release of unradiogenic Sr associated with arc weathering. The lag between minima in the marine Sr (38–40 Ma) and Os isotope records (34.2 Ma) is consistent with the expectation that uplift and erosion of the arc volcanics and associated sediments will precede intense ultramafic weathering.

The collision zone between India and Asia is an important region to seek evidence of intense ultramafic erosion during the late Eocene. Though imprecise chronologies preclude assessing detrital sources during the specific late Eocene time interval of interest here, provenance studies of Paleocene to Eocene clastic deposits of the Himalaya show that lithic fragments are commonly arc-derived, and occasionally ophiolitic [41,42]. Weathering of ultramafic rocks (Jijal and Sapat) associated the with accreted Kohistan arc within the Indus drainage basin in northern Pakistan may have contributed to the late Eocene $^{187}Os/^{188}Os$ minimum. This terrane currently resides in the Indus suture zone. It was accreted onto Eurasia in the late Cretaceous and was subject to further tectonism during the collision of India in the Eocene [43]. Ultramafic erosional remnants further to the east, in India (Spontang), China (Tso Morari), and Tibet (Jungbwa), suggest that a much more extensive thrust sheet containing ultramafic rocks near its base likely was present at one time, but has been largely eroded. The Spongtang Ophiolite and the ultramafic rocks of Tso Morari [44] are associated with a second accreted arc complex, the Spong arc [45]. Like the Dras–Kohistan arc the Spong arc was obducted in the late Cretaceous and subject to intense uplift and erosion during the collision of India with Asia [45]. Little is known about the Jungbwa ophiolite other than that it is an extremely large klippe [46].

4.1.3.2. Increased influx of extraterrestrial material. The late Eocene minimum in the marine $^{187}Os/^{188}Os$ record could also be attributed to an increased influx of extraterrestrial material. Although this possibility was discounted by Turekian and Pegram [9], it is important to carefully consider this possibility because it would imply that the excursion in seawater Os isotope composition is unrelated to changes in chemical weathering. It is well-known that episodes of increased influx of extraterrestrial material to the Earth can also produce excursions to low seawater $^{187}Os/^{188}Os$ [18,47], as illustrated by the sharp minimum in $^{187}Os/^{188}Os$ in LL44-GPC3 at the K–T boundary (Fig. 1). The Massignano Os isotope data disprove the hypothesis that the late Eocene dip in the marine Os record is synchronous with the late Eocene impacts and the episode of increased ^{3}He flux, because the lowest $^{187}Os/^{188}Os$ ratios lag

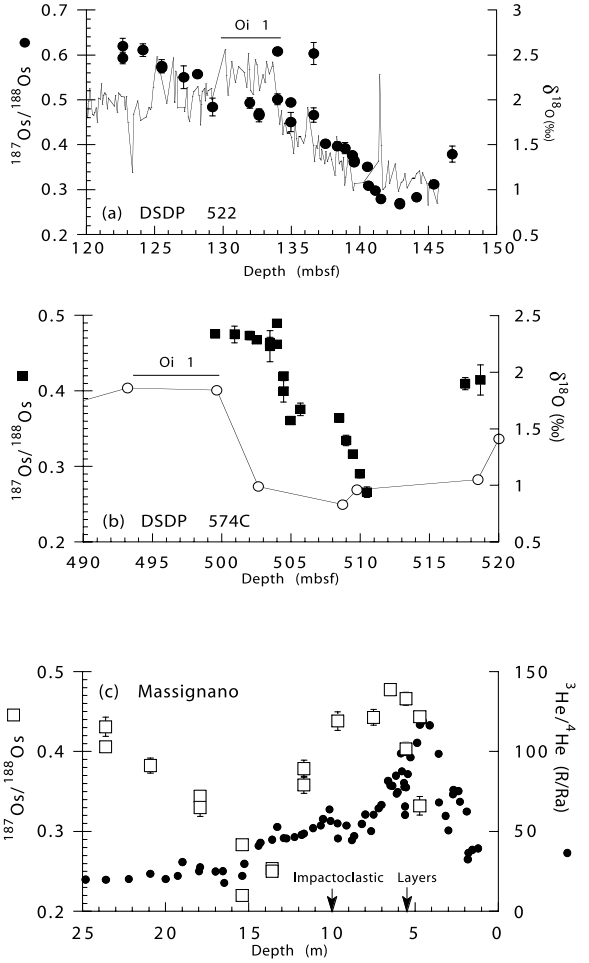

Fig. 2. Osmium isotope data from DSDP Site 522 in the South Atlantic (a), DSDP 574C in the Equatorial Pacific (b), and the Massignano section in the Italian Apennines (c) plotted vs. depth in core or section. In DSDP 522 (panel a) oxygen isotope ratios measured in the benthic foraminifer *Cibicidoides* spp. [5] show that seawater $^{187}Os/^{188}Os$ rose significantly during the growth and decay of the first major Antarctic ice sheet, but was relatively stable during the period of maximum ice volume (Oi1). Low-resolution benthic foraminiferal oxygen isotope data [61] and Os isotope data from DSDP 574C (panel b) show a similar pattern to DSDP 522 for the initiation of the Oi1 glaciation. Osmium isotope data from the Massignano section (panel c) show that lowest $^{187}Os/^{188}Os$ lags the episode of maximum ^{3}He flux, as indicated by largest $^{3}He/^{4}He$ ratio [8] and known late Eocene impacts [6,7].

the time of maximum ^{3}He flux by roughly 1.5 Myr (Fig. 2c). This confirms the He–Os relationship documented in LL44-GPC3 [9]. Moreover, the total duration of the Os isotope excursion is greater than 1 Myr. Given the short marine residence time of Os (approximately 50 kyr [37]) this is far too long to be associated with a single impact event. Instead, it implies a more protracted period of Os delivery, analogous to the episode of increased ^{3}He flux, but shifted in time 1.5 Myr later. We suggest that the episode of increased influx of ^{3}He and the excursion to low $^{187}Os/^{188}Os$ ratios may be causally related. Poynting–Robertson (P–R) drag is believed to control mean lifetime of interplanetary dust particles, and this process causes small particles to spiral Sun-ward more rapidly than larger particles [48]. Thus P–R drag provides a mechanism for the physical separation of the small-size fraction (<20 μm) of cosmic dust that carries ^{3}He to the Earth [49] and from the larger-size fraction, 100–200 μm, that represents the majority of the mass of interplanetary dust particles and the bulk of the Os flux [50] as they spiral through Earth-crossing orbits toward the Sun. The P–R lifetimes of the small-particle fraction that carries ^{3}He to the Earth are on the order of 10^{4}–10^{5} yr, implying relatively rapid delivery to the Earth after their production. In contrast, P–R drag calculations for 100 μm particles yield lifetime estimates close to 10^{6} yr [51]. Million-year lifetimes are consistent with exposure ages determined by ^{10}Be and ^{26}Al in large (approximately 500–700 μm) cosmic spherules from Antarctica [52], suggesting that the 1.5 Myr lag between excursions in the He and Os isotope records is not too long to result from P–R drag. In addition, the estimated relative magnitudes of the integrated excess ^{3}He and cosmic Os fluxes are within a factor of two: based on the model calculations described above, the average increase in cosmic Os flux is 6.5-fold relative to modern cosmic Os flux [50] for a period of 1.6 Myr, while the average increase in ^{3}He flux is two to three-fold relative to early Oligocene ^{3}He flux for a period of 2.4 Myr [8]. Thus we retain increased cosmic dust as an alternative hypothesis to the putative ultramafic erosional event described above to explain the late Eocene excursion in the marine Os isotope record. This possibility warrants further investigation because such a protracted episode of increased cosmic dust influx

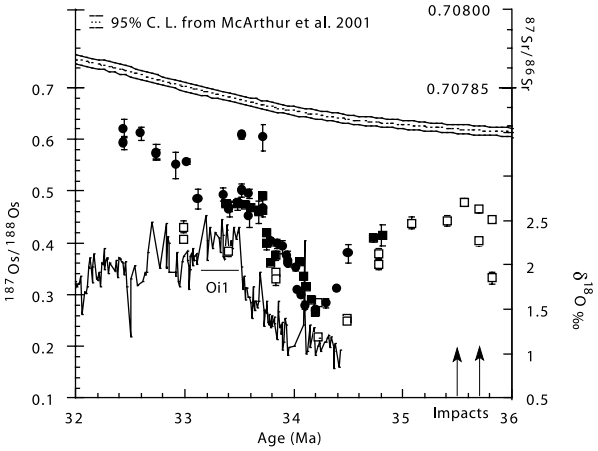

Fig. 3. Osmium isotope data from Fig. 2 are plotted vs. age. Models used to convert depth to age for both Site 522 [5] and Massignano [8] are based on magnetostratigraphy. The age model used for Hole 574C is based on the E–O boundary as defined by Thomas [28] and an assumed sedimentation rate of 1.33 cm/kyr. Note the pronounced minimum in $^{187}Os/^{188}Os$ close to 34.2 Ma, and the similarity of this composite record to the E–O portion of the low-resolution LL44-GPC3 record (Fig. 1). The oxygen isotope record shown is from Site 522 [5] and the Sr isotope curve is a best fit [40] to a composite data set.

might influence Earth's climate. Some possible connections between changes in cosmic dust flux and Earth's climate are described by [53].

4.2. *Chemostratigraphic potential of the late Eocene $^{187}Os/^{188}Os$ minimum*

Regardless of the cause of the late Eocene minimum in the seawater Os isotope record this feature provides a valuable tool for global correlation because its timing so closely precedes the Oi1 event (Figs. 2 and 3). This is particularly true in pelagic clay sequences because they lack most of the microfossils commonly used to constrain depositional ages. We use the eolian grain size record from LL44-GPC3 (Fig. 1) to illustrate the utility of Os isotope stratigraphy in pelagic clays. This record makes a pronounced shift to larger ϕ values, corresponding to smaller grain size, close to 18 m depth in the core. This change in grain size is interpreted as evidence of diminished wind intensity during the unusual warmth of the late Paleocene and early Eocene [54]. Close to the E–O boundary eolian grain size begins to increase, a change that has been attributed to more vigorous atmospheric circulation [55]. The $^{187}Os/^{188}Os$ minimum in LL44-GPC3 is shallower than the transition to increasing eolian grain size, requiring that this shift in grain size occurred before 34.2 Ma. The most recent biostratigraphic age assignments placed this transition in the early Oligocene [56]. If grain size variations do reflect changes in atmospheric circulation, then this change in age assignment is significant because it

Table 2
Estimates of Paleogene seawater Os isotope balance

	Riverine ^{188}Os flux (mol/yr)	Riverine $^{187}Os/^{188}Os$	Seawater (st. st.) $^{187}Os/^{188}Os$
Present-day seawater (after [62]	210	1.4	1.07
Paleogene 1 (decreased Os flux)	63	1.4	0.71
Paleogene 2 (best estimate)	67.5	0.81	0.45

Assumed input of unradiogenic Os is 75 mol/yr and $^{187}Os/^{188}Os = 0.13$ for all cases.
Steady-state $^{187}Os/^{188}Os$ calculated as $R_{sw} = R_r(f_r) + R_u(1-f_r)$, where f_r is the ratio of river flux of ^{188}Os to the total flux of ^{188}Os. Subscripts sw, r and u refer to seawater, riverine and unradiogenic, respectively.

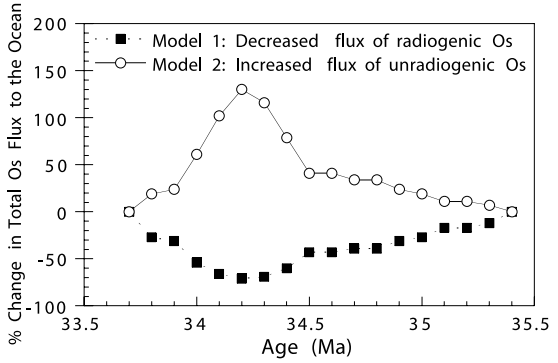

Fig. 4. Two different models of changing Os flux to illustrate two potential explanations of the late Eocene excursion to low $^{187}Os/^{188}Os$ ratios. The model curves are calculated to match the $^{187}Os/^{188}Os$ curve (Fig. 3) estimated at 100 kyr intervals. Flux changes are calculated as a series of steady-state balances starting from estimated pre-excursion conditions (Table 2). Model 1 assumes that the only change in Os inputs to the ocean is a decrease in the flux of riverine Os to the ocean, holding unradiogenic input equivalent to modern values (see Table 2 for the relevant equations). Model 2 assumes that the pre-excursion Os flux to the oceans is augmented by a flux of unradiogenic Os, $^{187}Os/^{188}Os = 0.13$ (see text for the relevant equation). Both calculations assume a transient perturbation in Os flux such that it returns to the pre-excursion steady state at 33.7 Ma.

implies that patterns of atmospheric circulation in the Northern Hemisphere as recorded by LL44-GPC3 were shifting to patterns characteristic of cooler–drier climate in advance of major Antarctic glaciation.

4.3. The Os isotope record of early Oligocene glaciation

The roughly 30% increase in long-term seawater $^{187}Os/^{188}Os$ that takes place across the E–O transition appears in the LL44-GPC3 record (Fig. 1) as a step-like increase punctuated by the late Eocene minimum. In our higher-resolution record it is clear this rise in seawater $^{187}Os/^{188}Os$ from the late Eocene minimum spans at least 1.5 Myr (Fig. 3). Comparison of the DSDP 522 Os isotope record to benthic foraminiferal $\delta^{18}O$ data [5], a proxy record for global ice volume, from the same core shows a gross positive correlation between $^{187}Os/^{188}Os$ and $\delta^{18}O$ (Fig. 2a). However, as discussed above, this initial increase corresponds to the recovery of seawater $^{187}Os/^{188}Os$ from the late Eocene minimum to $^{187}Os/^{188}Os$ ratios more typical of the Paleogene (0.4–0.45). Consequently, it is unclear to what extent growing ice sheets and the associated drop in sea level might have contributed to rising seawater $^{187}Os/^{188}Os$ prior to Oi1 [2].

In the Site 522 record (Fig. 2a) $^{187}Os/^{188}Os$ stabilizes at values of 0.45 prior to the abrupt rise in $\delta^{18}O$ that marks the final phase of Oi1 ice sheet growth [5]. The Site 574 record (Fig. 2b) also records the plateau in $^{187}Os/^{188}Os$ at 0.45 and shows that it precedes the shift to higher $\delta^{18}O$ values in the Pacific as well. In the Site 522 record, increases in $^{187}Os/^{188}Os$ to ratios above the 0.45 plateau do not occur until after the shift to lower $\delta^{18}O$ values that mark the termination of Oi1. As Antarctic ice wanes and benthic $\delta^{18}O$ values decrease at approximately 33.2 Ma, seawater $^{187}Os/^{188}Os$ increases to 0.6, and correlates with higher $^{187}Os/^{188}Os$ in the LL44-GPC3 record. This indicates that radiogenic Os is released to seawater at an accelerated rate upon deglaciation.

Results from the study of Os release from a

Table 3
Sediment mass accumulation rate estimates used for burial flux calculations

	Dry bulk density (g/cm^3)	Sediment rate (cm/kyr)	Sediment burial flux ($g/(cm^2\ kyr)$)
Massignano (after [8])	2.5	0.7	1.75
Site 522[a], above 124.7 mbsf	1.22	0.93	1.14
Site 522[a], 134.25–124.7 mbsf	1.22	1.2	1.47
Site 522[a], below 124.7 mbsf	1.22	1.3	1.59
Hole 574C	1.12	1.2	1.49

[a] Dry bulk density estimates based on data from shipboard porosity and weight bulk density data. For accumulation rate estimates see text for Hole 574C, and [5] for Site 522.

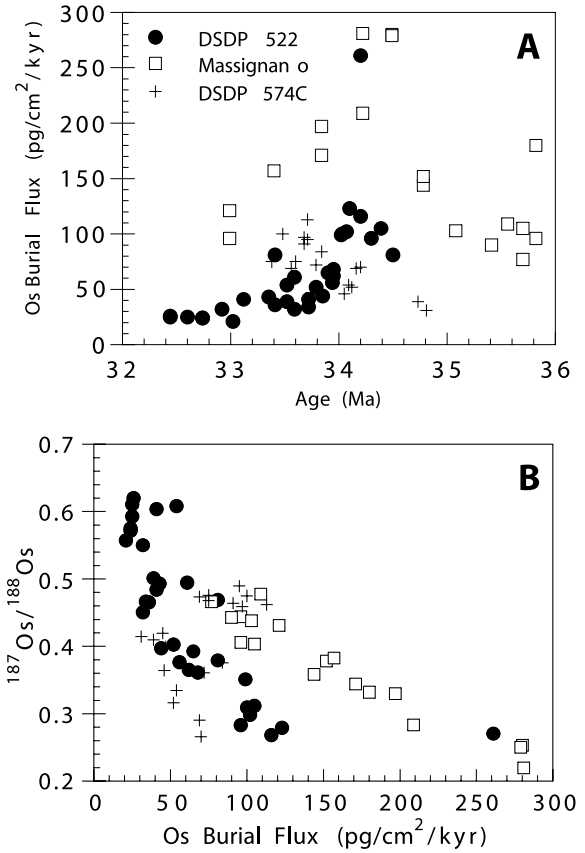

Fig. 5. Total Os burial fluxes plotted as a function of age (panel A). At Massignano and in DSDP 522, the maximum in Os burial flux occurs at 34.2 Ma. In DSDP 574C, there is a local maximum in Os burial at this time, with maximum Os burial fluxes in younger samples. Note the similarity between Os burial flux history at Massignano and DSDP 522 and model 2 in Fig. 4. Measured $^{187}Os/^{188}Os$ is anticorrelated with Os burial flux (panel B). At a given site the lowest $^{187}Os/^{188}Os$ generally occurs in sediments with largest Os burial flux. This is also consistent with interpreting the late Eocene $^{187}Os/^{188}Os$ minimum as the result of increased delivery of unradiogenic Os to the ocean.

chronosequence of glacial moraines [4] shows that rapid release of radiogenic Os can result from chemical weathering of young glacial deposits exposed by retreating ice. Specifically, this work and related studies demonstrate that young glacial moraines weather very rapidly, producing large fluxes of base cations [3] and preferential release of ^{187}Os [4] and ^{87}Sr [3]. The timing of the rise to $^{187}Os/^{188}Os$ from values close to 0.45 to ratios close to 0.6 is consistent with a scenario in which weathering of young glacial deposits produced by the retreating Antarctic ice sheet drives an increase in seawater $^{187}Os/^{188}Os$ ratios. It is important to note that the glacial weathering studies cited above indicate that the glacial moraines weather very rapidly during the first several thousand years, but that after 100 kyr the weathering rate decreases significantly. In contrast, the increase in seawater $^{187}Os/^{188}Os$ during the early Oligocene appears to be permanent. Spectral analyses of benthic oxygen isotope records [5] show clear evidence of orbital forcing after the Oi1 event. We suggest that the cyclic changes in ice volume regularly replenish the supply of freshly eroded material, allowing relatively higher fluxes of ^{187}Os to the ocean to be maintained once persistent glacial conditions are established.

Changes in weathering flux associated with the transition from greenhouse to icehouse conditions need not be limited to areas that are subject to glacial erosion. Paleosol records from the northwestern United States yield evidence of a distinct change in the style of weathering, and an increase in total weathering rates across the E–O transition [57]. Regardless of where changes in weathering are occurring, comparison of the Os and oxygen isotope records provides evidence of climatic controls on the release of ^{187}Os from continents across the E–O transition. This comparison suggests that increased continental weathering, as signaled by increasing seawater $^{187}Os/^{188}Os$, is driven by deglaciation following the Oi1 event, while peak glacial conditions, characterized by relatively constant $^{187}Os/^{188}Os$, are not. If increasing $^{187}Os/^{188}Os$ is indicative of an increase in chemical weathering flux upon the termination of Oi1, this suggests a coupling between chemical weathering and glaciation that allows deglacial drawdown of atmospheric CO_2 associated with increased silicate weathering rates to contribute ice-sheet stabilization. This idea is discussed further by Kump et al. [58].

Early Oligocene Os isotope variations help to resolve ambiguities associated with interpretations of the marine Sr isotope record. Osmium and Sr in average crustal material [59], dissolved riverine load [37,60], and weathering glacial debris [4] are all characterized by radiogenic isotope ratios, sug-

gesting that there is broad coherence in the weathering fluxes of Os and Sr. The marine residence time of osmium is two to three orders of magnitude shorter than that of Sr [37], allowing the Os isotopes to faithfully record abrupt changes in riverine flux that are strongly damped in the marine Sr isotope record. The increase in seawater $^{187}Os/^{188}Os$ associated with the termination of Oi1 supports the interpretations of previous investigators [10–12] that glaciation enhances the release of radiogenic Sr from continents and is at least partly responsible for rising seawater $^{87}Sr/^{86}Sr$ across the E–O transition.

Acknowledgements

We thank Tracy Abbruzzese for her excellent work in the lab and Jurek Blusztajn for help sparging. We are also grateful to Lary Ball and Dave Schneider for the work in the WHOI ICP-MS facility. Ken Farley kindly provided sample material from Massignano. All other sample material was provided by the Ocean Drilling Program. Ken Farley and Jim Zachos provided electronic versions of data files that have been replotted in this manuscript. Ken Miller and an anonymous reviewer offered critical comments that led to an improved manuscript. Peter Clift, Peter Kelemen and Mike Searle shared helpful ideas on the distribution of ultramafic rocks in the collision zone between India and Asia. Ellen Thomas provided valuable advice on the biostratigraphy of Hole 574C. Mukul Sharma directed us to the cosmogenic nuclide chronology work by Nishizumi et al. This work was supported by NSF award OCE-0118380. This is WHOI contribution No. 10,884.*[BOYLE]*

References

[1] W.J. Pegram, K.K. Turekian, The osmium isotopic composition change of Cenozoic sea water as inferred from a deep-sea core corrected for meteoritic contributions, Geochim. Cosmochim. Acta 63 (1999) 4053–4058.

[2] K.G. Miller, J.D. Wright, R.G. Fairbanks, Unlocking the ice house: Oligocene-Miocene oxygen isotopes, eustasy and margin erosion, J. Geophys. Res. 96 (1991) 6829–6848.

[3] J.D. Blum, The effect of late Cenozoic glaciation and tectonic uplift on silicate weathering rates and the marine $^{87}Sr/^{86}Sr$ record, in: W.F. Ruddiman (Ed.), Tectonic Uplift and Climate Change, Plenum Press, New York, 1997, pp. 259–288.

[4] B. Peucker-Ehrenbrink, J.D. Blum, The effects of global glaciation on the osmium isotopic composition of continental runoff and seawater, Geochim. Cosmochim. Acta 62 (1998) 3193–3203.

[5] J.C. Zachos, T.M. Quinn, K.A. Salamy, High-resolution (10^4 years) deep-sea foraminiferal stable isotope records of the Eocene-Oligocene climate transition, Paleoceanography 11 (1996) 251–266.

[6] R. Bottomley, R. Grieve, D. York, V.L. Masaitis, The age of the Popigai impact event and its relation to events at the Eocene/Oligocene boundary, Nature 388 (1997) 365–368.

[7] C. Koeberl, C.W. Poag, W.U. Reimold, D. Brandt, Impact origin of the Chesapeake Bay structure and the source of the North American tektites, Science 271 (1996) 1263–1266.

[8] K.A. Farley, A. Montanari, E.M. Shoemaker, C.S. Shoemaker, Geochemical evidence for a comet shower in the late Eocene, Science 280 (1998) 1250–1253.

[9] K.K. Turekian, W.J. Pegram, Os isotope record in a Cenozoic deep-sea core: Its relation to global tectonics and climate, in: W.F. Ruddiman (Ed.), Tectonic Uplift and Climate Change, Plenum Press, New York, 1997, pp. 383–397.

[10] R.L. Armstrong, Glacial erosion and the variable isotopic composition of strontium in sea water, Nat. Phys. Sci. 230 (1971) 132–133.

[11] K.G. Miller, M.D. Feigenson, J.D. Wright, B.M. Clement, Miocene isotope reference section, Deep Sea Drilling Project Site 608; an evaluation of isotope and biostratigraphic resolution, Paleoceanography 6 (1991) 33–52.

[12] J.C. Zachos, B.N. Opdyke, T.M. Quinn, C.E. Jones, A.N. Halliday, Early Cenozoic glaciation, Antarctic weathering, and seawater $^{87}Sr/^{86}Sr$; is there a link?, Chem. Geol. 161 (1999) 165–180.

[13] M.E. Raymo, W.F. Ruddiman, P.N. Froelich, The influence of late Cenozoic mountain building on ocean geochemical cycles, Geology 16 (1988) 649–653.

[14] M.E. Raymo, W.F. Ruddiman, Tectonic forcing of late Cenozoic climate, Nature 359 (1992) 117–122.

[15] A.K. Clymer, D.M. Bice, A. Montanari, Shocked quartz from the late Eocene; impact evidence from Massignano, Italy, Geology 24 (1996) 483–486.

[16] O. Pierrard, E. Robin, R. Rocchia, A. Montanari, Extraterrestrial Ni-rich spinel in upper Eocene sediments from Massignano, Italy, Geology 26 (1998) 307–310.

[17] R. Oxburgh, Variations in the osmium isotope composition of seawater over the past 200,000 years, Earth Planet. Sci. Lett. 159 (1998) 183–191.

[18] B. Peucker-Ehrenbrink, G. Ravizza, A.W. Hofmann, The

marine $^{187}Os/^{186}Os$ record of the past 80 million years, Earth Planet. Sci. Lett. 130 (1995) 155–167.
[19] G. Ravizza, Variations of the $^{187}Os/^{186}Os$ ratio of seawater over the past 28 million years as inferred from metalliferous carbonates, Earth Planet. Sci. Lett. 118 (1993) 335–348.
[20] D.N. Reusch, G. Ravizza, K.A. Maasch, J.D. Wright, Miocene seawater $^{187}Os/^{188}Os$ ratios inferred from metalliferous carbonates, Earth Planet. Sci. Lett. 160 (1998) 163–178.
[21] A. Montanari, F. Asaro, H.V. Michel, J.P. Kennett, Iridium anomalies of late Eocene age at Massignano (Italy), and ODP Site 689B (Maud Rise, Antarctic), Palaios 8 (1993) 420–437.
[22] G.S. Odin, A. Montanari, The Eocene-Oligocene boundary at Massignano (Ancona, Italy); a potential stratotype for the Eocene-Oligocene boundary. In: I. Premoli Silva, R. Coccioni, A. Montanari (Eds.). The Eocene-Oligocene boundary in the Marche-Umbria Basin (Italy), Int. Union Geol. Sci., Comm. Stratigr. Ancona, 1988, pp. 253–263.
[23] L. Lanci, W. Lowrie, A. Montanari, Magnetostratigraphy of the Eocene/Oligocene boundary in a short drill-core, Earth Planet. Sci. Lett. 143 (1996) 37–48.
[24] K.J. Hsue, J.L. LaBrecque, M.F. Carman Jr., A.M. Gombos Jr., A.-M. Karpoff, J.A. McKenzie, S.F. Percival Jr., N.P. Petersen, K.A. Pisciotto, R.Z. Poore, E. Schreiber, L. Tauxe, P. Tucker, H.J. Weissert, M.G. Bailey, Site 522, DSDP Init. Report 73 (1984) 187–270.
[25] P. Hartl, L. Tauxe, C. Constable, Early Oligocene geomagnetic field behavior from Deep Sea Drilling Project Site 522, J. Geophys. Res. B 98 (1993) 19649–19665.
[26] C.H. Lear, H. Elderfield, P.A. Wilson, Cenozoic deep-sea temperatures and global ice volumes from Mg/Ca in benthic foraminiferal calcite, Science 287 (2000) 269–272.
[27] L.A. Mayer, F. Theyer, J.A. Barron, D.A. Dunn, T. Handyside, S. Hills, I. Jarvis, C.A. Nigrini, N.G. Pisias, A. Pujos, T. Saito, P.M. Stout, E. Thomas, N. Weinreich, R.H. Wilkens, M.G. Bailey, Site 574, DSDP Init. Report 85 (1985) 225–329.
[28] E. Thomas, Late Eocene to Recent deep-sea benthic foraminifers from the central Equatorial Pacific Ocean, DSDP Init. Report 85 (1985) 655–694.
[29] A. Pujos, Cenozoic nannofossils, central Equatorial Pacific, Deep Sea Drilling Project Leg 85, DSDP Init. Report 85 (1985) 581–607.
[30] J.A. Barron, Late Eocene to Holocene diatom biostratigraphy of the Equatorial Pacific Ocean, Deep Sea Drilling Project Leg 85, DSDP Init. Report 85 (1985) 413–456.
[31] C.A. Nigrini, Radiolarian biostratigraphy in the central Equatorial Pacific, Deep Sea Drilling Project Leg 85, DSDP Init. Report 85 (1985) 511–551.
[32] D.R. Hassler, B. Peucker-Ehrenbrink, G.E. Ravizza, Rapid determination of Os isotopic composition by sparging OsO_4 into a magnetic-sector ICP-MS, Chem. Geol. 166 (2000) 1–14.
[33] G. Ravizza, D. Pyle, PGE and Os isotopic analyses of single sample aliquots with NiS fire assay preconcentration, Chem. Geol. 141 (1997) 251–268.
[34] F. Marcantonio, K.K. Turekian, S. Higgins, R.F. Anderson, M. Stute, P. Schlosser, The accretion rate of extraterrestrial ^{3}He based on oceanic ^{230}Th flux and the relation to Os isotope variation over the past 200,000 years in an Indian Ocean core, Earth Planet. Sci. Lett. 170 (1999) 157–168.
[35] F.M. Richter, D.B. Rowley, D.J. DePaolo, Sr isotope evolution of seawater: the role of tectonics, Earth Planet. Sci. Lett. 109 (1992) 11–23.
[36] K. Wallmann, Controls on the Cretaceous and Cenozoic evolution of seawater composition, atmospheric CO_2 and climate, Geochim. Cosmochim. Acta 65 (2001) 3005–3025.
[37] S. Levasseur, J.L. Birck, C.J. Allegre, The osmium riverine flux and the oceanic mass balance of osmium, Earth Planet. Sci. Lett. 174 (1999) 7–23.
[38] M. Sharma, G.J. Wasserburg, A.W. Hofmann, G.J. Chakrapani, Himalayan uplift and osmium isotopes in oceans and rivers, Geochim. Cosmochim. Acta 63 (1999) 4005–4012.
[39] D.N. Reusch, K.A. Maasch, The transition from arc volcanism to exhumation, weathering of young Ca, Mg, Sr silicates, and CO_2 drawdown, Tectonic boundary conditions for climate reconstructions, Oxford Monogr. Geol. Geophys. 39 (1998) 261–276.
[40] J.M. McArthur, R.J. Howarth, T.R. Bailey, Strontium isotope stratigraphy; LOWESS Version 3; best fit to the marine Sr-isotope curve for 0-509 Ma and accompanying look-up table for deriving numerical age, J. Geol. 109 (2001) 155–170.
[41] P.D. Clift, N. Shimizu, G.D. Layne, J.S. Blusztajn, C. Gaedicke, H.U. Schlueter, M.K. Clark, S. Amjad, Development of the Indus Fan and its significance for the erosional history of the western Himalaya and Karakoram, Geol. Soc. Am. Bull. 113 (2001) 1039–1051.
[42] Y. Najman, E. Garzanti, Reconstructing early Himalayan tectonic evolution and paleogeography from Tertiary foreland basin sedimentary rocks, northern India, Geol. Soc. Am. Bull. 112 (2000) 435–449.
[43] M.P. Searle, M. Asif Khan, J.E. Fraser, S.J. Gough, M. Qasim Jan, The tectonic evolution of the Kohistan-Karakoram collision belt along the Karakoram Highway transect, North Pakistan, Tectonics 18 (1999) 929–949.
[44] S. Guillot, K.H. Hattori, J. de Sigoyer, T. Naegler, A.-L. Auzende, Evidence of hydration of the mantle wedge and its role in the exhumation of eclogites, Earth Planet. Sci. Lett. 193 (2001) 115–127.
[45] R.I. Corfield, M.P. Searle, R.B. Pedersen, Tectonic setting, origin, and obduction history of the Spontang Ophiolite, Ladakh Himalaya, NW India, J. Geol. 109 (2001) 715–736.
[46] J.P. Burg, A. Bonneville, A. Beaud, J. Girardeau, J. Marcoux, First results on the broadest ophiolitic klippe in a collision belt: the Jungbwa thrustsheet, North Tibet, EOS Trans. AGU 72 (1991) 288.

[47] T. Meisel, U. Krahenbühl, M.A. Nazarov, Combined osmium and strontium isotopic study of the Cretaceous-Tertiary boundary at Sumbar, Turkmenistan: A test for an impact vs. a volcanic hypothesis, Geology 23 (1995) 313–316.
[48] J.A. Burns, P.L. Lamy, S. Soter, Radiation forces on small particles in the solar system, Icarus 40 (1979) 1–48.
[49] K.A. Farley, S.G. Love, D.B. Patterson, Atmospheric entry heating and helium retentivity of interplanetary dust particles, Geochim. Cosmochim. Acta 61 (1997) 2309–2316.
[50] B. Peucker-Ehrenbrink, G. Ravizza, The effects of sampling artifacts on cosmic dust flux estimates; a reevaluation of nonvolatile tracers (Os, Ir), Geochim. Cosmochim. Acta 64 (2000) 1965–1970.
[51] S.F. Dermott, K. Grogan, D.D. Durda, J. Sumita, T.J.J. Kehoe, S.J. Kortenkamp, M.C. Wyatt, Orbital evolution of interplanetary dust, in: E.E. Grün, B.A.S. Gustafson, S.F. Dermott, H. Fechtig (Eds.), Interplanetary Dust, Springer, Berlin, 2001, pp. 569–640.
[52] K. Nishizumi, J.R. Arnold, D.E. Brownlee, M.W. Caffee, R.C. Finkle, R.P. Harvey, Beryllium-10 and aluminum-26 in individual cosmic spherules from Antarctica, Meteoritics 30 (1995) 728–732.
[53] R.A. Muller, Glacial cycles and interplanetary dust, in: B. Peucker-Ehrenbrink, B. Schmitz (Eds.), Accretion of Extraterrestrial Matter Throughout Earth's History, Kluwer Academic/Plenum, New York, 2001, pp. 143–162.
[54] D.K. Rea, Changes in atmospheric circulation during the latest Paleocene and earliest Eocene epochs and some implications for the global climate regime, in: Late Paleocene-Early Eocene; Climatic and Biotic Events in the Marine and Terrestrial Records, Columbia University Press, New York, 1998, pp. 118–123.
[55] D.K. Rea, M. Leinen, T.R. Janecek, Geologic approach to the long-term history of atmospheric circulation, Science 227 (1985) 721–725.
[56] M.D. Gottfried, P.S. Doyle, W.R. Riedel, Advances in ichthyolith stratigraphy of the Pacific Neogene and Oligocene, Micropaleontology 30 (1984) 71–85.
[57] E.A. Bestland, Weathering flux and CO_2 consumption determined from Palaeosol sequences across the Eocene-Oligocene transition, Palaeogeogr. Palaeoclimatol. Palaeoecol. 156 (2000) 301–326.
[58] L.R. Kump, S.L. Brantley, M.A. Arthur, Chemical weathering, atmospheric CO_2, and climate, Annu. Rev. Earth Planet. Sci. 28 (2000) 611–667.
[59] B. Peucker-Ehrenbrink, B.-m. Jahn, Rhenium-osmium isotope systematics and platinum group element concentrations: Loess and the upper continental crust, Geochem. Geophys. Geosyst. 2 (2001) 10.1029/2001GC000172.
[60] M.R. Palmer, J.M. Edmond, Controls over the strontium isotope composition of river water, Geochim. Cosmochim. Acta 56 (1992) 2099–2111.
[61] K.G. Miller, E. Thomas, Late Eocene to Oligocene benthic foraminiferal isotopic record, Site 574, Equatorial Pacific, DSDP Init. Report 85 (1985) 771–777.
[62] B. Peucker-Ehrenbrink, G. Ravizza, The marine osmium isotope record, Terra Nova 12 (2001) 205–219.